

THE MAJORANA ^{76}Ge DOUBLE-BETA DECAY PROJECT

C.E. Aalseth¹, D. Anderson¹, F.T. Avignone III², A. Barabash³, T.W. Bowyer¹, R.L. Brodzinski¹, V. Brudanin⁴, J.I. Collar⁵, P.J. Doe⁶, S. Egorov⁴, S.R. Elliott⁶, H.A. Farach², R. Gaitskell⁷, D. Jordan¹, O. Kochetov⁴, S. Kononov³, R. Kouzes¹, H.S. Miley¹, W.K. Pitts¹, J.H. Reeves¹, R.G.H. Robertson⁶, V. Sandukovsky⁴, E. Smith¹, V. Stekhanov³, R.C. Thompson¹, W. Tornow^{8,9}, V. Umatov³, R.A. Warner¹, J. Webb¹⁰, J. Wilkerson⁶, and A. Young¹¹
(The Majorana Collaboration)

The Majorana Experiment is a next-generation ^{76}Ge double-beta decay search. It will employ 500 kg of Ge, isotopically enriched to 86% in ^{76}Ge , in the form of ~ 200 detectors in a close-packed array for high granularity. Each crystal will be electronically segmented, with each region fitted with pulse-shape analysis electronics. A half-life sensitivity is predicted of 4.2×10^{27} y or $\langle m_\nu \rangle \leq 0.02 - 0.07$ eV, depending on the nuclear matrix elements used to interpret the data.

¹Pacific Northwest National Laboratory, Richland, WA 99352, USA

²University of South Carolina, Columbia, SC 29208, USA

³Institute for Theoretical and Experimental Physics, Moscow 117259, Russia

⁴Joint Institute for Nuclear Research, Dubna, Russia

⁵University of Chicago, Chicago, IL, USA

⁶University of Washington, Seattle, WA, USA

⁷Brown University, Providence, RI, USA

⁸Triangle Universities Nuclear Laboratory, Durham, NC, USA

⁹Duke University, Durham, NC, USA

¹⁰New Mexico State University, NM, USA

¹¹North Carolina State University, Raleigh, NC, USA

1 Introduction

Neutrino oscillation experiments have produced “smoking guns” for non-zero neutrino mass in the solar neutrino deficit[1], in the excess of $p(\bar{\nu}_e, e^+)n$ reactions in the LSND experiment[2], and from the zenith-angle dependence of the electron-to-muon event ratio in the Super-Kamiokande (SK) data[3] (see also [4, 5, 6]). The results of reactor neutrino experiments[7] constrain the disappearance of $\bar{\nu}_e$ well enough to imply that the SK data are dominated by $\nu_\mu \rightarrow \nu_\tau$ ($\bar{\nu}_\mu \rightarrow \bar{\nu}_\tau$) oscillations, with only a minimal oscillation to electron-type neutrinos, since they show $\bar{\nu}_e$'s do not oscillate as readily as required by the SK data for $\nu_\mu \rightarrow \nu_e$ or $\bar{\nu}_\mu \rightarrow \bar{\nu}_e$ oscillations to have a significant role.

While the interpretation of the SK data in terms of neutrino oscillations is widely accepted, there were questions concerning the interpretation of the LSND data as evidence of $\bar{\nu}_\mu \rightarrow \bar{\nu}_e$ oscillations. Some doubt existed that the standard solar model was accurate enough to support the conclusion that there was really a deficit of solar neutrinos. When the results of all solar neutrino experiments are considered, there is no scenario in which these data are compatible with the standard solar model unless the flux of ν_e from the sun oscillates partially into other ν -flavors to which the experiments are not sensitive.

On 17 July 2001, however, the Sudbury Neutrino Observatory (SNO) collaboration settled this issue. They published results from the direct measurement of the rate of the reaction $d(\nu_e, e^-)pp$ from solar neutrinos[8]. The neutrino flux implied by these data was compared with that from neutral-current neutrino-electron elastic scattering data from SK. It was concluded that there is an active, non-electron-flavor neutrino component in the solar neutrino flux, and that the total flux of active neutrinos from the ^8B branch is in close agreement with the standard solar model of Bahcall and his co-workers[1]. The standard solar model is thereby confirmed, and the case for neutrino oscillations is now compelling.

A remaining question is that of the LSND indication of $\bar{\nu}_\mu \rightarrow \bar{\nu}_e$ oscillations. All attempts to incorporate these results in the same analysis with the solar neutrino and atmospheric neutrino experiments fail in any scenario involving only three neutrino flavors.

Accepting that now both solar and atmospheric neutrino experiments give clear evidence for neutrino oscillations, there are only two conclusions to be drawn from the LSND data. Either the excess events from the reaction $p(\bar{\nu}_e, e^+)n$ in the LSND is due to phenomena other than $\bar{\nu}_\mu \rightarrow \bar{\nu}_e$ oscillation, or that there must exist a fourth generation of neutrinos “sterile” with respect to “normal” weak interactions[9]. To insist on accepting one or the other of these options at the present time is to accept an unsubstantiated theoretical prejudice. This issue is still very much an open one. The MiniBooNE experiment will settle this issue; however, it will be a search for $\nu_\mu \rightarrow \nu_e$, not $\bar{\nu}_\mu \rightarrow \bar{\nu}_e$ as in LSND.

While an unambiguous interpretation of all of the neutrino oscillation experiments is not yet possible, it is abundantly clear that neutrinos exhibit properties not included in the standard model, namely mass and flavor mixing. Accordingly, sensitive searches for neutrinoless double-beta decay ($0\nu \beta\beta$ -decay) are more important than ever. Experiments with kilogram quantities of germa-

nium, isotopically enriched in ^{76}Ge , have thus far proven to be the most sensitive, specifically the Heidelberg-Moscow[10] and IGEX[11] experiments. The lower limits in half-life sensitivities are: 1.9×10^{25} y[10] and 1.6×10^{25} y[11]. A new generation of experiments will be required to make significant improvements in sensitivity, as discussed later.

Petcov and Smirnov[12] showed that both MSW and vacuum oscillation solutions of the solar neutrino problem can be compatible with $0\nu\beta\beta$ -decay driven by an effective Majorana electron-neutrino mass in the range 0.1 to 1.0 eV. The interpretation of all the neutrino oscillation data together, as discussed later, implies a range that could be between 5 and 10 times lower. The exploration of such a range will require next-generation experiments. Some that are being proposed are: CAMEO[13], CUORE[14], EXO[15], GENIUS[16], Majorana[17], and MOON[18].

2 Neutrinoless Double-Beta Decay

Neutrinoless double-beta decay is a process by which two neutrons in a nucleus beta decay by exchanging a virtual Majorana neutrino, each emitting an electron. This violates lepton number conservation ($\Delta l = 2$). There are many reviews on the subject[19, 20, 21, 22].

The decay rate for the process involving the exchange of a Majorana neutrino can be written as follows:

$$\lambda_{\beta\beta}^{0\nu} = G^{0\nu}(E_0, Z)\langle m_\nu \rangle^2 |M_f^{0\nu} - (g_A/g_V)M_{GT}^{0\nu}|^2. \quad (1)$$

In equation 1, $G^{0\nu}$ is the two-body phase-space factor including coupling constants, $M_f^{0\nu}$ and $M_{GT}^{0\nu}$ are the Fermi and Gamow-Teller nuclear matrix elements respectively, and g_A and g_V are the axial-vector and vector relative weak coupling constants, respectively. The quantity $\langle m_\nu \rangle$ is the effective Majorana neutrino mass given by:

$$\langle m_\nu \rangle \equiv \left| \sum_{k=1}^{2n} \lambda_k^{CP} (U_{lk}^L)^2 m_k \right|, \quad (2)$$

where λ_k^{CP} is the CP eigenvalue associated with the k^{th} neutrino mass eigenstate (± 1 for CP conservation), U_{lk}^L is the (l, k) matrix element of the transformation between flavor eigenstates $|\nu_l\rangle$ and mass eigenstates $|\nu_k\rangle$ for left handed neutrinos,

$$|\nu_l\rangle = \sum U_{lk}^L |\nu_k\rangle, \quad (3)$$

and m_k is the mass of the k^{th} neutrino mass eigenstate.

The effective Majorana neutrino mass, $\langle m_\nu \rangle$, is directly derivable from the measured half-life of the decay as follows:

$$\langle m_\nu \rangle = m_e (F_N T_{1/2}^{0\nu})^{-1/2} eV, \quad (4)$$

where $F_N \equiv G^{0\nu} |M_f^{0\nu} - (g_A/g_V) M_{GT}^{0\nu}|^2$, and m_e is the electron mass. This quantity derives from nuclear structure calculations and is model dependent.

The most sensitive experiments thus far utilize germanium detectors isotopically enriched in ^{76}Ge from 7.78% abundance to $\sim 86\%$. Germanium detector experiments were started with natural abundance detectors by Fiorini, et al., in Milan[22], evolving over the years to the first experiments with small isotopically enriched detectors, and finally to the two present multi-kilogram isotopically-enriched ^{76}Ge experiments: Heidelberg-Moscow[10] and IGEX[11]. Reference [10] has about four times the exposure as reference [11] with limits of similar magnitude. This strongly implies that experiments with on the order of 100 moles of ^{76}Ge have reached the point of diminishing returns.

Where should the field of double-beta decay go from here? Suppose the observed neutrino oscillations of atmospheric neutrinos and solar neutrinos are considered. What probable range of $\langle m_\nu \rangle$ is implied? Would it be large enough to allow the direct observation of $0\nu \beta\beta$ -decay? If so, what technique would be the best for a possible discovery experiment?

3 Theoretical Motivation and Probable Neutrino Scenarios

The SK data imply maximal mixing of ν_μ with ν_τ with $\delta m_{23}^2 \simeq 3 \times 10^{-3} \text{ eV}^2$. The solar neutrino data from SK and from SNO also imply that the small mixing angle solution to the solar neutrino problem is disfavored, so that δm^2 (solar) $\simeq (10^{-5} - 10^{-4}) \text{ eV}^2$. Based on these interpretations, one probable scenario for the neutrino mixing matrix has the following approximate form:

$$\begin{pmatrix} \nu_e \\ \nu_\mu \\ \nu_\tau \end{pmatrix} = \begin{pmatrix} 1/\sqrt{2} & 1/\sqrt{2} & 0 \\ -1/\sqrt{2} & 1/\sqrt{2} & 1/\sqrt{2} \\ 1/\sqrt{2} & -1/\sqrt{2} & 1/\sqrt{2} \end{pmatrix} \begin{pmatrix} \nu_1 \\ \nu_2 \\ \nu_3 \end{pmatrix} \quad (5)$$

The neutrino masses can be arranged in two hierarchical patterns in which $\delta m_{31}^2 \simeq \delta m_{32}^2 \sim 3 \times 10^{-3} \text{ eV}^2$, and $\delta m_{21}^2 \sim (10^{-5} - 10^{-4}) \text{ eV}^2$. With available data, it is not possible to determine which hierarchy, $m_3 > m_1(m_2)$, or $m_1(m_2) > m_3$, is the correct one, nor is the absolute value of any of the mass eigenstates known.

The consideration of reactor neutrino and atmospheric neutrino data together strongly implies that the atmospheric neutrino oscillations are very dominantly $\nu_\mu \rightarrow \nu_\tau$ ($\bar{\nu}_\mu \rightarrow \bar{\nu}_\tau$), which implies, as seen from equation 5, that ν_e is very dominantly a mixture of ν_1 and ν_2 . In this case there will be one relative CP phase, ϵ , and equation 2 reduces to the approximate form:

$$\langle m_\nu \rangle = \frac{1}{2}(m_1 + \epsilon m_2), \quad (6)$$

where the large mixing angle solution of the solar neutrino problem implies

$$(m_2^2 - m_1^2) = (10^{-5} - 10^{-4}) \text{ eV}^2. \quad (7)$$

Assuming that $\epsilon \simeq +1$, and that neutrinos are Majorana particles, then it is very probable that $0\nu\beta\beta$ -decay is driven by an effective electron neutrino mass between 0.01 eV and the present bound from ^{76}Ge experiments. Consider the relation

$$T_{1/2}^{0\nu} = \frac{(\ln 2)Nt}{c}, \quad (8)$$

where N is the number of parent nuclei, t is the counting time, and c is the maximum number of counts that can be attributed to $0\nu\beta\beta$ -decay. To improve the sensitivity to $\langle m_\nu \rangle$ by a factor of 10^2 from the present ~ 1 eV to 0.01 eV, one must increase the quantity Nt/c by a factor of 10^4 . The quantity N can feasibly be increased by a factor of $\sim 10^2$ over present experiments, implying t/c must also be improved by a similar amount. Since the present counting times are probably about a factor of 5 less than a practical counting time, the background should be reduced by at least a factor of 20 below present levels. A further reduction is probably feasible and should be pursued.

4 The Majorana ^{76}Ge $0\nu\beta\beta$ -Decay Experiment

The Majorana experiment is proposed for a US deep underground laboratory, and requires very little R&D. It stands on the technical shoulders of the IGEX experiment and other previous successful double-beta decay and low-background experiments. Furthermore, new segmented Ge detector technology has recently become commercially available, while Pacific Northwest National Laboratory (PNNL)/University of South Carolina (USC) researchers have developed new pulse-shape discrimination techniques.

The IGEX experiment terminated with 117 mole-years of data with an average background of 0.06 c/keV/kg/y in the later data sets. The resulting half life is 1.6×10^{25} y and its implied bounds on $\langle m_\nu \rangle$ are shown in Table 1.

The Majorana experiment represents a great increase in Ge mass over IGEX with new segmented Ge detectors and the newest electronic systems for pulse-shape discrimination. It is conceived to be 500 kg of Ge detectors, fabricated from Ge isotopically enriched to 86% in ^{76}Ge . The typical detector size will be approximately 2.4 kg, requiring about 200 detectors. Below is presented the projected sensitivity for such an array, shown in an artist's conception in Figure 1.

The array will have a fiducial mass of 500 kg, containing $N = 3.43 \times 10^{27}$ atoms of ^{76}Ge ; a counting time of 10 years, and an energy resolution of 3.0 keV FWHM. The starting background assumed is that achieved by IGEX, prior to pulse-shape discrimination, which was $b_0 = 0.2$ counts/keV/kg/y at the $0\nu\beta\beta$ -decay energy of 2039 keV. This background was achieved at 4000 mwe and was completely accounted for as the decay of cosmogenic isotopes in the germanium[24]. The decay of ^{68}Ge (270.8-day half-life) and ^{60}Co (5.7-year half-life) over the 10-year counting period, combined with estimates of reduced above-ground cosmogenic activation and additional decay during detector construction, reduces this background by an overall factor of about twenty, com-

pared to the IGEX background mentioned. This reduces the expected background rate to 0.01 c/keV/kg/y.

The optimum energy window for a simple Poisson analysis is 2.8σ of the Gaussian peak (83.8%), or 3.57 keV. The total number of background counts in this window around 2039 keV over a 10-year period would then be

$$b \cdot \Delta E \cdot M \cdot t = (0.01 \text{ c/keV/kg/y})(3.57 \text{ keV})(5000 \text{ kg} \times \text{y}) = 178 \quad (9)$$

prior to data cuts.

Above-ground experiments by the PNNL/USC collaborators demonstrate that new pulse-shape discrimination methods have an acceptance fraction for internal cosmogenic backgrounds of no more than 0.265. Monte Carlo simulations demonstrate detector segmentation will allow an additional cut with an acceptance fraction for internal cosmogenic backgrounds of no more than 0.138. An example of the effect of segmentation on internal cosmogenic background in the 2 MeV region-of-interest is shown in Figure 2. Applying both of these orthogonal cuts is expected to reduce the background to 6.5 remaining events. If the background in the region is featureless in energy, a simple Poisson analysis yields a limit of 6 events as the number of $0\nu \beta\beta$ -decay events consistent with the background (90% CL).

The two cuts discussed do not have 100% efficiency for accepting $0\nu \beta\beta$ -decay events. The pulse-shape discrimination has a measured single-site-event acceptance fraction of 0.802. The detector-segmentation cut has a calculated single-site-event acceptance fraction of 0.907. The total counting efficiency is then 0.727. Accordingly the sensitivity is projected as:

$$T_{1/2}^{0\nu}(\text{sens}) \simeq \frac{(0.727)(.693)(3.43 \times 10^{27}) 10}{6} \simeq 4.2 \times 10^{27} \text{ y.} \quad (10)$$

This analysis does not account for the fact that the close-packed granularity of ~ 200 crystals will allow further cuts against multiply-scattered background events. The background computed above is therefore conservative. The resulting upper bounds on $\langle m_\nu \rangle$ are shown in Table 1 and, discarding an unfavored QRPA form factor, range from 0.02 eV to 0.07 eV.

Table 1: Nuclear structure factor F_N and Majorana neutrino mass parameters $\langle m_\nu \rangle$ for $T_{1/2}^{0\nu} = 1.6 \times 10^{25}$ y and for 4.2×10^{27} y.

F_N, yr^{-1}	Model [reference]	$\langle m_\nu \rangle$ (eV)	$\langle m_\nu \rangle$ (eV)
1.56×10^{-13}	Shell Model[25]	0.32	0.020
9.67×10^{-15}	QRPA[26]	1.3	0.080
1.21×10^{-13}	QRPA[27]	0.37	0.023
1.12×10^{-13}	QRPA[28]	0.38	0.024
1.41×10^{-11}	Shell Model[29]	1.08	0.067

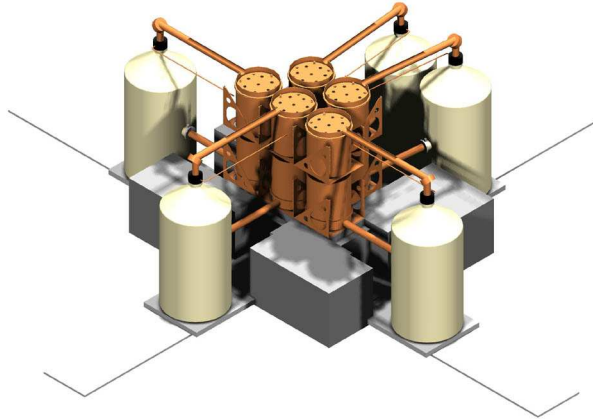


Figure 1: An artist's conception of the Majorana array of Ge detectors using present cryostat technology. Other, more granular arrays will also be investigated.

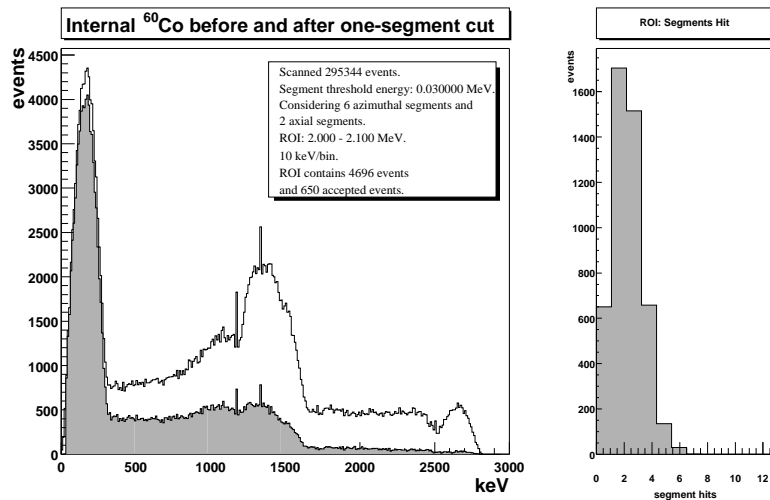


Figure 2: Monte Carlo simulation of internal ^{60}Co background. The plot on the left shows the spectrum before and after a one-segment-only cut is applied. The plot on the right displays a histogram of the number of segments in which energy was deposited for internal ^{60}Co background events falling in a 2.0–2.1 MeV region-of-interest.

5 Recent Progress in Ge Detector Technology

Majorana is not simply a volume expansion of IGEX. It must have superior background rejection. Because it has been conclusively shown that the limiting background in at least some previous experiments has been cosmogenic activation of the germanium itself, it is necessary to mitigate those background sources. Cosmogenic activity fortunately has certain factors which discriminate it from the signal of interest. For example, while $0\nu\beta\beta$ -decay would deposit 2 MeV between two electrons in a small, perhaps 1 mm³ volume, internal ⁶⁰Co decay deposits about 318 keV (endpoint) in beta energy near the decaying atom, while simultaneous 1173 keV and 1332 keV gammas can deposit energy elsewhere in the crystal, most probably both in more than one location, for a total energy capable of reaching the 2039 keV region-of-interest. A similar situation exists for internal ⁶⁸Ge decay. Thus deposition-location multiplicity distinguishes double-beta decay from the important long lived cosmogenics in germanium. Isotopes such as ⁵⁶Co, ⁵⁷Co, ⁵⁸Co, and ⁶⁸Ge are produced at a rate of roughly 1 atom per day per kilogram on the earth's surface[24]. Only ⁶⁰Co and ⁶⁸Ge have both the energy and half-life to be of concern.

To pursue the multiplicity parameter, two approaches are possible. First, the detector current pulse shape carries with it the record of energy deposition along the electric field lines in the crystal; crudely speaking, the radial dimension of cylindrical detectors. This information may be exploited through pulse-shape discrimination. Second, the electrical contacts of the detector may be divided to produce independent regions of charge collection.

By segmenting the inner contact into two (axial) parts and the outer contact into 6 (azimuthal) parts, as shown in Figure 3, multiplicity data can be obtained. The Monte-Carlo simulation data set shown in Figure 2 is based on this configuration and shows that internal highly-multiple backgrounds like ⁶⁰Co can be strongly suppressed at 2038 keV. The internal ⁶⁰Co modeled in the figure is produced by cosmic-ray neutrons during the preparation of the detector, accumulating after the last crystal-growth step. Its elimination by segmentation and pulse shape discrimination is crucial. Beyond this simple segmentation cut, it may be possible to use the signals derived from segments seeing no net charge, adjacent to a segment seeing net charge, to locate a single-site deposition in the axial and azimuthal coordinates of the crystal or to distinguish a single-site deposition from a multiple one. This possible technique is not currently included in sensitivity calculations. Intrinsic n-type Ge detectors with segmented electrical contacts are now available commercially. After Monte Carlo studies and discussions with detector manufacturers, the general configuration shown in Figure 3 is believed to be optimal for balancing background reduction, cost and production efficiency.

The development of the pulse-shape discrimination technique used in the sensitivity calculation arose from earlier work comparing experimental pulses with completely simulated ones. After repeated trials with fully simulated pulses, this early method was set aside due to the unpredictable effect of preamplifier noise levels and the unacceptable sensitivity of the resulting cuts to the detector

Twelve Section Segmented Ge Detector

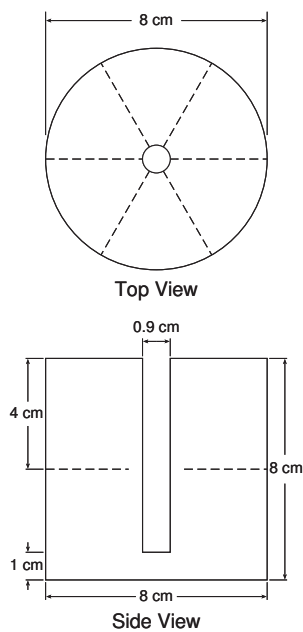


Figure 3: The geometry of the segmented detectors planned for the Majorana experiment.

and charge-collection model. For example, the parameters needed to correctly simulate pulses include the space-charge density remaining after crystal depletion. This is most often poorly known and represents essentially a set of free parameters for the simulation. The operating voltage of the crystal, which may require variation during the crystal lifetime, is also critically important to the fidelity of simulated pulse formation. Thus, any system built upon the accuracy of predicted or modeled pulse-shapes was found less than optimum for cutting efficacy and fragile with respect to long-term maintenance.

A much-superior pulse-shape discrimination method was constructed using a set of parameters calculated from each pulse. The parameters for a single pulse are compared to a distribution collected from a calibration source of interest. Those which conform to a large degree are kept; those which do not are discarded. The acceptance ratio is adjusted during pulse post-processing to optimize cut efficacy. The strength of this approach is that no set of simulated pulses need be maintained; no space charges need be known. It is only required that calibration data be obtained before and after any voltage change, a procedure which is required in any case to periodically check detector gain.

To summarize, new techniques depend entirely on experimental calibration and do not utilize pulse-shape libraries. The ability of these techniques to be easily calibrated for individual detectors makes them practical for large detector arrays.

This development was in large part due to a shift in thinking about digitization, earlier digitization had been done with an 8-bit digitizer sampling as frequently as 500 MHz. Theory held that by oversampling, the energy resolution afforded by analog acquisition could be achieved, which is well-matched to 14-bits. However, measurement of actual preamplifier bandwidth showed that there is no more than 25 MHz of information in the signal. Thus, emerging hardware for 40-MHz 12-bit acquisition, such as the Digital Gamma Finder (DGF) produced by X-Ray Instrumentation Associates (XIA)[30], allows both a high-resolution energy value and a high-fidelity waveform to be acquired in a single, lower cost, and highly stable electronics chain. After acquiring a detector preamplifier pulse, all subsequent operations on the signal are performed digitally. The particular unit used in pulse-shape discrimination development is the 4-channel DFG-4C, developed and manufactured by XIA.

The DGF-4C has 4 independent, 40 MHz, 12-bit analog-to-digital converters (ADCs). The ADCs are followed by First-in, First-out (FIFO) buffers capable of storing 1024 ADC values for a single event. In parallel with each FIFO is a programmable digital filter and trigger logic. The digital filter and trigger logic for each channel is combined into a single Field Programmable Gate Array (FPGA). Analog input data are continuously digitized and processed at 40 MHz.

Experimental example pulses are shown in Figure 4. An example single-site event from the 1592 keV double-escape peak of the ^{208}Tl 2615 keV line is shown as the top signal. The bottom signal is an example multi-site pulse from the full-energy peak of the ^{212}Bi line at 1620 keV.

The DGF-4C is a smart filter of incoming pulses. If, for example, a signal has a pulse-width incompatible with the usual collection time of 200-1000 ns, or is oscillatory (like microphonic noise), the trigger filter can be programmed to reject it. This feature can be used to allow the very low energy thresholds required in Dark Matter searches as well as eliminating a broad spectrum of very-low-rate artificial pulses from high voltage leaks and electromagnetic interference that can appear in the energy region of $0\nu\beta\beta$ -decay.

Calibration for single-site event pulses is trivially accomplished by collecting pulses from thorium ore; the 2614.47-keV gamma ray from ^{208}Tl produces a largely single-site double-escape peak at 1592.47 keV. The PSD discriminator is then calibrated to the properties of the double-escape peak. A slightly improved double-escape peak can be made from the ^{26}Al gamma ray of 2938.22-keV. The double-escape appears at 1916.22 keV, only about 120 keV away from the expected region of interest for $0\nu\beta\beta$ -decay. The obvious and direct use of pulse-shape discrimination and segmentation is the rejection of cosmogenic pulses in the germanium itself. However, the approach should be also effective on gamma rays from the shielding and structural materials.

The effects as background of neutrons of both high energy (cosmic muon generated) and low energy (fission and (α,n) from rock) are under consideration

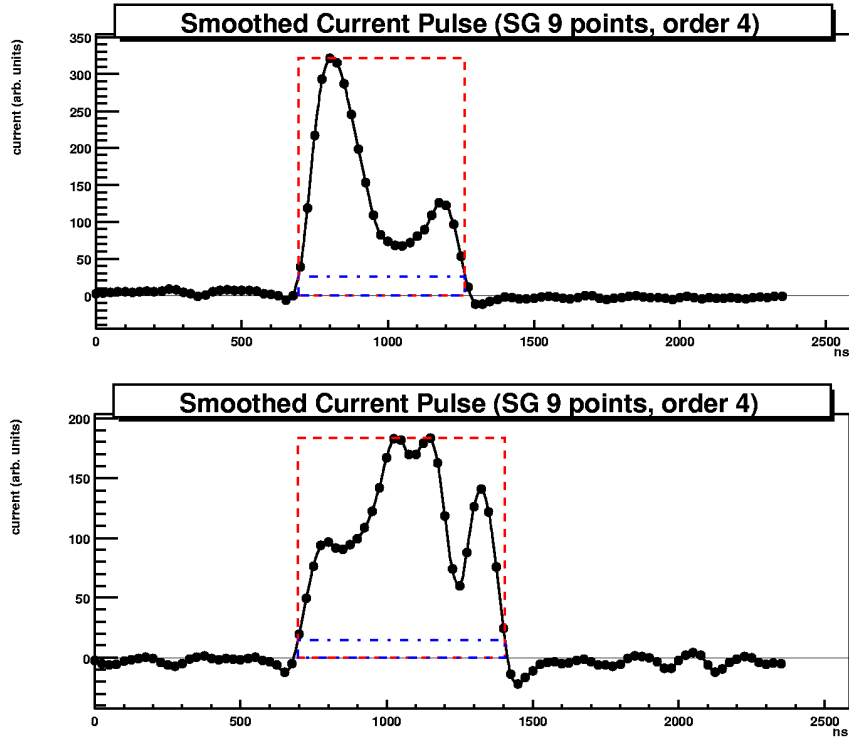


Figure 4: Reconstructed current signal from a 1592-keV double-escape-peak event (top) and a 1620.6-keV full-energy gamma peak event (bottom). Horizontal scale spans 2500 ns.

as well. The segmentation and granularity of the detectors will provide some protection from this lower-order background. These neutrons could also produce other unwanted activities. For instance, ^3H and ^{14}C can be produced in nitrogen from high and low energy neutrons, respectively. Fortunately, Majorana detectors will not be surrounded by nitrogen at high density.

In conclusion, the Majorana project has been designed in a compact, modular way such that it can be built and operated with high confidence in the approach and the technology. The initial years of construction will allow alternate cooling methods to be employed if they have an advantage and should they be shown to overcome long-term concerns due to surface contamination, muon-induced ions, and diffusion. The technology supporting Majorana signal-processing-based background rejection is ready and shows promise of future improvements. The technology of radiopure copper production has improved steadily since the last IGEX system, in which copper support materials played no measurable radiological role. Finally, those who enrich germanium have also

expressed their enthusiasm and support for the project. Thus, the Majorana project is poised ready to begin operations toward determining the effective Majorana mass of the electron neutrino.

References

- [1] J.N. Bahcall, Centennial Lecture, Neutrino-2000, Nucl. Phys. B (Proc. Suppl.) **91**, 9 (2001).
- [2] G.B. Mills, Nucl. Phys. B (Proc. Suppl.) **91**, 198 (2001).
- [3] H. Sobel (for the Super-Kamiokande Collaboration), Nucl. Phys. B (Proc. Suppl.) **91**, 127 (2001); Y. Fukuda, *et al.*, Phys. Rev. Lett. **81**, 1562 (1998); **82**, 1810 (1999).
- [4] Y. Fukuda, *et al.*, Phys. Lett. **B 335**, 237 (1994).
- [5] D. Casper, *et al.*, Phys. Rev. Lett. **66**, 2561 (1991); R. Becker-Szendy, *et al.*, Phys. Rev. **D 46**, 3720 (1992).
- [6] S. Ahlen, *et al.*, Phys. Rev. Lett. **72**, 608 (1994).
- [7] M. Apollonio, *et al.*, Phys. Lett. **B 420**, 397 (1998); Phys. Lett. **B 466**, 415 (1999). The CHOOZ Collaboration, and F. Boehm, *et al.*, Nucl. Phys. **91**, 91 (2001). The Palo Verde Collaboration.
- [8] Q.R. Ahmad, *et al.*, Phys. Rev. Lett. **87**, 071301-1 (2001).
- [9] J. Ellis (Summary Talk) Neutrino-2000, Nucl. Phys. B (Proc. Suppl.) **91**, 503 (2001).
- [10] L. Baudis, *et al.*, Phys. Rev. Lett. **83**, 41 (1999); see also F.T. Avignone III, C.E. Aalseth, and R.L. Brodzinski, Phys. Rev. Lett. **85**, 465 (2000). (The value of 1.9×10^{25} years is the new official Heidelberg Value Presented by H.V. Klapdor-Kleingrothaus at NANP-2001, June 2001, Dubna, Russia).
- [11] C.E. Aalseth, *et al.*, (IGEX Collaboration), Yad. Phys. **63**, 1299 (2000); D. Gonzales, Nucl. Phys. B (Proc. Suppl.) **87**, 278 (2000).
- [12] S.T. Petcov and A.Yu. Smirnov, Phys. Lett. **B 322**, 109 (1994).
- [13] G. Bellini, *et al.*, IFN Preprint arXiv: nucl-ex/0007012, 11 July 2000, SIS-Pubblicazioni dei Laboratori di Frascati.
- [14] A. Allesandrello, *et al.*, Phys. Lett. **B 420**, 109 (1998); Nucl. Phys. **B 87**, 78 (2000).
- [15] M. Danilov, *et al.*, Phys. Lett. **B 480**, 12 (2000).
- [16] H.V. Klapdor-Kleingrothaus, J. Helmig, and M. Hirsch, J.Phys. G: Nucl. Part. Phys. **24**, 483 (1998).

- [17] L. De Braekeleer (for the Majorana Collaboration), Proc. Carolin Conf. on Neutrino Physics (Columbia SC USA, 10-12 March 2000), eds. J.N. Bahcall, W.C. Haxton, K. Kubodera, and C.P. Poole, World Scientific.
- [18] H. Ejiri, *et al.*, Phys. Rev. Lett. **85**, 2917 (2000).
- [19] H. Primakoff and S.P. Rosen, Rep. Prog. Phys. **22**, 121 (1959); Phys. Rev. **184**, 1925 (1969).
- [20] W.C. Haxton and G.J. Stevenson Jr., Prog. Part. Nucl. Phys. **12**, 409 (1984); F.T. Avignone III and R.L. Brodzinski, Prog. Part. Nucl. Phys. **21**, 99 (1988); M. Moe and P. Vogel, Ann. Rev. Nucl. Part. Sci **44**, 247 (1994).
- [21] A. Morales, Nucl. Phys. B (Proc. Suppl.) **77**, 335 (1999); H. Ejiri, Phys. Rept. C (2000), Int. J. Mod. Phys. E6, 1 (1997); V. Tretyak and Y. Zdesenko, At. Data, Nucl. Data Tables **61**, 43 (1995).
- [22] E. Fiorini *et al.*, Phys. Lett. **25 B**, 602 (1967); Lett. Nuovo Cimento **3**, 149 (1970).
- [23] J.N. Bahcall and M.H. Pinsonneault, Rev. Mod. Phys. **67**, 781 (1995). For an update on uncertainties in the models see J.N. Bahcall, S. Basu, and M.H. Pinsonneault, Phys. Lett. **B 433**, 1 (1998).
- [24] R. L. Brodzinski, H. S. Miley, J. H. Reeves, and F. T. Avignone, III. Low-background germanium spectrometry – the bottom line three years later. *Journal of Radioanalytical and Nuclear Chemistry*, 193(1):61–70, 1995.
- [25] W.C. Haxton and G.T. Stephenson Jr., Prog. Part. Nucl. Phys. **12**, 409 (1984).
- [26] P. Vogel and M.R. Zirnbauer, Phys. Rev. Lett. **57**, 3148 (1986); J. Engel, P. Vogel, and M.R. Zirnbauer, Phys. Rev. **C 37**, 731 (1988).
- [27] O. Civitarese, A. Faessler, and T. Tomoda, Phys. Lett. **B 194**, 11 (1987); T. Tomoda and A. Faessler, Phys. Lett. **B 199**, 475 (1987).
- [28] K. Muto, E. Bender, and H.V. Klapdor, Z.Phys. **A 177**, 334 (1989). The matrix elements used in Table 1 are from A. Standt, K. Muto, and H.V. Klapdor, Europhys. Lett. **13**, 31 (1990).
- [29] E. Caurier, *et al.*, Phys. Rev. Lett. **77**, 1954 (1996).
- [30] B. Hubbard-Nelson, M. Momayezi and W.K. Warburton, Nucl. Instr. and Meth. in Physics Research **A 422**, 411 (1999).